

# Intrashell transitions in Rydberg atom-ion collisions: Quantum and classical approaches

A. K. Kazansky and V. N. Ostrovsky

*Institute of Physics, The University of St. Petersburg, 198904 St. Petersburg, Russia*

(Submitted 12 March 1996)

*Zh. Éksp. Teor. Fiz.* **110**, 1988–2002 (December 1996)

Intrashell transitions in Rydberg atom induced by distant collisions with charged particle imply close coupling of  $n^2$  channels which correspond to the (quasi) degenerate states of Rydberg atom with the same principal quantum number  $n$ . In the case when the Rydberg atom is initially in the  $ns$  state very simple explicit analytical expressions are obtained for the quantum amplitudes of transitions into the final spherical or parabolic states. They are derived in the dipole approximation and are based on the Fock  $O(4)$  symmetry group for the hydrogen atom. The semiclassical limit of the solution is compared with our previous classical trajectory (pseudo) Monte Carlo treatment of the problem. The Monte Carlo approach is shown to give very accurate results for the transition cross sections. Thus the binning procedure conventionally used in the Monte Carlo calculations is justified. © 1996 American Institute of Physics. [S1063-7761(96)00512-4]

## 1. INTRODUCTION

In addition to their value for various applications (such as the kinetics of low-temperature plasma and astrophysics), studies of processes involving Rydberg atoms are of considerable fundamental interest. In particular, collision of a Rydberg atom with a charged particle is one form of the fundamental three-body Coulomb problem in atomic physics (for a review see Ref. 1). When a charged particle approaches the Rydberg atom, it efficiently induces transitions within the manifold of degenerate states (with fixed principal quantum number  $n$ ) even at large interparticle distances. These processes can be also referred to as  $l$ -changing transitions ( $nl_0 \rightarrow nl$ ). Note however that the initial and/or final states could be alternatively labelled by other quantum numbers (among which the parabolic basis is the most natural one). Resonant intrashell transitions have the largest cross sections<sup>2</sup> and strongly influence all other inelastic processes which occur at smaller separations (such as excitation and charge exchange). These transitions always comprise an essential part of the collision process; as an example we refer to the radiative stabilization of Rydberg states in double charge exchange<sup>3</sup> and to manifestations of the intrashell transitions in ZEKE spectroscopy of large molecules which are actively discussed in the current literature (see, e.g., Refs. 4). No less important is another fundamental aspect of the problem; the processes with Rydberg atoms are well known to be convenient objects for study of the relation between quantum and classical methods of description.

It is generally recognized that for higher collision velocities the dipole-allowed transitions  $\Delta l = \pm 1$  dominate. As  $v$  decreases, the processes with larger  $|\Delta l|$  become more and more significant. This is interpreted as a series of stepwise transitions in a single collision event. In order to describe them within quantum mechanics, some sort of coupled-channel method is required. When the reduced collision velocity  $v/n$  is not large, it is necessary to include in the calculations all the atomic states with the same principal quantum

number  $n$  as that in the initial Rydberg state. The amount of states inside the hydrogenic shell ( $\sim n^2$ ) is prohibitively large for numerical calculations when typical Rydberg atoms are concerned. For instance, in a recent paper by Sun and MacAdam<sup>2</sup> the Rydberg states with  $n=26$  or 28 were employed.

The classical approach in atomic physics inevitably implies calculation of individual classical trajectories for various initial conditions which are randomly chosen from the classical ensemble corresponding to the initial quantum state. This scheme is commonly referred to as the Classical Trajectory Monte Carlo (CTMC) method. The outcome of the collision is described in terms of continuous observables (for example, the final electron orbital momentum  $l$ ). It is related to the final quantum states using some binning procedure. Namely, the continuous scale of  $l$  is subdivided into intervals (bins); each bin is related to some integer quantum number  $l$ .<sup>5</sup> For intrashell transitions the CTMC calculations require very large amount of numerical work, which apparently explains why CTMC calculations have not yet been carried out for this process. Note that the intrashell transitions are induced by the long-range dipole interaction, which increases the necessary numerical work in both quantum and classical approaches.

Actually the exact explicit solution of the quantum problem (within some natural assumptions outlined in the next section) was obtained quite long ago.<sup>6</sup> However the form of the results was complicated and cumbersome. This was the reason why in fact they were applied to practical calculations only in the simplest case  $n=2$ . In an alternative approach Beigman and Syrkin<sup>7</sup> used a special *ad hoc* averaging procedure to reduce the number of quantum coupled equations to  $n$  and considered some approximate methods of solution for the resulting system of equations. The numerical results obtained in<sup>7</sup> are in reasonable agreement with the recent experimental data.<sup>2</sup> However, the averaging procedure is difficult to justify theoretically. Additionally, this approach does not allow one to calculate distributions over the azimuthal

quantum number  $m$  or over the parabolic quantum numbers.

The present study was stimulated by two recent developments.

1. Sun and MacAdam<sup>2</sup> carried out measurements for the  $l$ -mixing process with Rydberg atoms having principal quantum number  $n=26$  or 28. For high  $n$  the calculation of finite sums discussed above becomes quite tedious. It is equally important that the simplicity of the derivation is in some controversy with relatively complicated final formulae. It should be stressed also that the current experimental data refer to relatively small values of final quantum numbers  $l$ , whereas for low collision velocities the states with large  $l$  are populated efficiently.

2. In order to interpret and complement the experimental data, Kazansky and Ostrovsky<sup>8</sup> developed a theory in which the Rydberg electron is treated as a classical particle; all other physical inputs used in Ref. 6 above were retained. This approach could be classified as pseudo-CTMC scheme. It gave unexpectedly simple formulae for the final-state distributions over the parabolic or spherical integral of motion (subsequently converted to distributions over the related quantum numbers using the binning procedure).

The object of the present study is to find the quantum analogues to the simple results of the classical theory. After that we trace the transition from quantum theory to the classical limit in order to analyze the applicability of the classical approach and the role of quantum effects. This analysis allows us to justify the binning procedure employed in CTMC.

The simplifications achieved in the earlier classical and in the present quantum treatments are related to the particular but very important case when the electron is initially in the  $s$ -state.<sup>1)</sup> It should be stressed that realistic  $l$ -mixing experiments nowadays are carried out with low- $l$  Rydberg atoms in initial states<sup>2</sup> which could be effectively treated as  $s$ -states.<sup>8</sup>

It has to be emphasized that the possibility of obtaining simple analytical quantum solutions has a deep group-theoretical foundation. Namely, it stems from the fact that the symmetry of the discrete states of the hydrogen atom is described by the four-dimensional rotation group  $O(4)$ , as discovered by Fock.<sup>9</sup>

## 2. BASIC IDEAS

We consider a collision between a Rydberg atom in a state with the principal quantum number  $n$  and an ion with charge  $Z$ . The relative motion of the colliding particles is treated by means of classical mechanics. This allows us to determine the time-dependence for the internuclear vector  $\mathbf{R}$  directed from the Rydberg atom nucleus to the incident ion. The electron wavefunction  $\psi(\mathbf{r}, t)$  obeys the time-dependent non-stationary Schrödinger equation<sup>2)</sup>

$$i \frac{\partial \psi}{\partial t} = \mathcal{H}(t) \psi \quad (1)$$

with the Hamiltonian

$$\mathcal{H}(t) = \mathcal{H}_0 - \frac{Z}{|\mathbf{R}(t) - \mathbf{r}|} + \frac{Z}{R(t)}, \quad \mathcal{H}_0 = -\frac{1}{2} \nabla_r^2 - \frac{1}{r}, \quad (2)$$

where  $\mathbf{r} = \{x, y, z\}$  is the electron vector relative to the Rydberg atom nucleus. The unperturbed motion of the electron is governed by the purely Coulomb Hamiltonian  $\mathcal{H}_0$ ; the effect of the non-Coulomb core is included below.

Since the resonance transitions have very large cross sections, we can employ the long-range dipole approximation for the interaction

$$-\frac{Z}{|\mathbf{R}(t) - \mathbf{r}|} + \frac{Z}{R(t)} \approx -Z \frac{\mathbf{r} \cdot \mathbf{R}(t)}{R(t)^3}. \quad (3)$$

In the collision plane the internuclear vector  $\mathbf{R}$  is characterized by the azimuthal angle  $\Phi(t)$  ( $\Phi(-\infty) = 0$ ). Following Demkov *et al.*<sup>6</sup> we introduce a rotating coordinate system<sup>3)</sup> with the axis  $z' = z$  perpendicular to the collision plane and the axis  $x'$  directed along the vector  $\mathbf{R}(t)$ . Transition to this frame is achieved by applying the operator for a finite rotation to the wave function (together with a simple phase transformation):

$$\psi' = \exp[-iE_n t + i\Phi(t)\hat{l}_z] \psi, \quad (4)$$

$$i \frac{\partial \psi'}{\partial t} = \mathcal{H}'(t) \psi', \quad (5)$$

$$\mathcal{H}'(t) = -Z \frac{x'}{R(t)^2} - \frac{\mathcal{L}_z}{\mu R(t)^2} \hat{l}_z. \quad (6)$$

Here  $E_n = -1/(2n^2)$  is the unperturbed Rydberg electron energy,  $\mathbf{l}$  is the vector operator of the electron orbital momentum,  $\mathcal{L}$  is the vector of the angular momentum for the relative motion of the colliding particle (which is perpendicular to the collision plane,  $\mathcal{L} = \mathcal{L}_z = \mu R^2 d\Phi/dt$ ), and  $\mu$  is the reduced mass,  $\hat{l}_z = \hat{l}_z'$ . The operator  $\mathcal{H}'$  coincides with the Hamiltonian of the hydrogen atom in uniform electric and magnetic fields

$$\mathcal{H}' = \mathbf{E} \cdot \mathbf{r}' + \frac{1}{2c} \mathbf{H} \cdot \mathbf{l}' \quad (7)$$

( $c$  is the velocity of light). The effective magnetic field is equivalent to the Coriolis force acting in the rotating frame; note that the diamagnetic term ( $\sim H^2$ ) does not appear in the frame transformation. The electric field  $\mathbf{E}$  is directed along the  $x'$  axis and has the magnitude  $E = -Z/R^2(t)$ . The effective magnetic field is directed along the  $z'$  axis with the magnitude  $(1/2c)H = -\mathcal{L}/[\mu R^2(t)]$ .

Thus the problem is reduced to the description of the excited hydrogen atom in perpendicular electric and magnetic fields. It can be solved explicitly both in classical and quantum mechanics.

The classical problem (with time-independent fields having arbitrary directions) was considered by Epstein<sup>11</sup> and Pauli<sup>12</sup> (more precisely, these authors treated the problem within the old quantum mechanics, which implied analysis of the slow evolution of the classical trajectories; see also Born<sup>13</sup>). The electron orbit was characterized by the orbital momentum  $\mathbf{L}$  and the Runge-Lenz vector  $\mathbf{A}$  directed from the atomic nucleus towards the orbit aphelion. In classical mechanics the Runge-Lenz vector  $\mathbf{A}$  is proportional to the electron coordinate  $\mathbf{r}(t)$  averaged over the fast motion of the electron in its unperturbed elliptic orbit:  $\langle \mathbf{r} \rangle = 3n\mathbf{A}/2$ . The

slow evolution of the trajectories can be described as precession of the vectors  $\mathbf{I}_1=(\mathbf{L}+\mathbf{A})/2$  and  $\mathbf{I}_2=(\mathbf{L}-\mathbf{A})/2$ . The axes of precession are directed respectively along the vectors

$$\boldsymbol{\omega}_1 = \frac{3}{2} n\mathbf{E} + \frac{1}{2c} \mathbf{H}, \quad \boldsymbol{\omega}_2 = \frac{3}{2} n\mathbf{E} - \frac{1}{2c} \mathbf{H}. \quad (8)$$

The precession frequencies are equal to  $\omega_1$  and  $\omega_2$ . The precessions are uniform in time.

The quantum version of the theory was developed by Demkov *et al.*<sup>14</sup> Here we emphasize that the classical averaging over the fast electron motion corresponds in quantum mechanics to the approximate reduction of the problem to the subspace of degenerate electron states having the same principal quantum number  $n$ .

The vector operators  $\mathbf{I}_1$  and  $\mathbf{I}_2$  possess all properties of the angular momentum operators in quantum mechanics. They are independent, i.e., commute with each other and have fixed length:  $\mathbf{I}_1^2 = \mathbf{I}_2^2 = j(j+1)$  with  $j=(n-1)/2$ . The unperturbed hydrogenic states can be labelled by the quantum numbers  $i_1$  and  $i_2$  which are eigenvalues for the projections of the operator vectors  $\mathbf{I}_1$  and  $\mathbf{I}_2$  on some axis. This representation differs only in notation from the standard representation of the parabolic quantum numbers  $n_1, n_2, m$  (subject to the constraint  $n_1 + n_2 + |m| + 1 = n$ ), since  $m = i_1 + i_2$ ,  $n_1 - n_2 = i_1 - i_2$ . The connection between the parabolic  $(n_1, n_2, m)$  basis and the spherical  $(l, m)$  basis is universally known. The preceding explanation presupposes that the vectors  $\mathbf{I}_1$  and  $\mathbf{I}_2$  are quantized along the same axis in space. Generally this constraint can be lifted, since the operators are independent. The necessity to quantize these operators along different axes in space appears just in the problem of the hydrogen atom in the crossed electric and magnetic fields. Namely, the eigenstates of the Hamiltonian (7) (reduced to  $n$ -subspace) correspond to quantization of the operator  $\mathbf{I}_1$  along the  $\boldsymbol{\omega}_1$ -axis and the operator  $\mathbf{I}_2$  along the  $\boldsymbol{\omega}_2$ -axis.

Returning to the collision problem, we have to stress that here we encounter time-dependent effective electric and magnetic fields. The general solution of the problem with time-dependent fields cannot be obtained in analytical form. However the effective fields specific to the collision problem have two important properties:

- (i) their directions are fixed in space in the rotating frame;
- (ii) they have the same time dependence governed by the factor  $R^{-2}(t)$ .

Due to the first property in the course of the collision the precession axes  $\boldsymbol{\omega}_1$  and  $\boldsymbol{\omega}_2$  do not change their directions (in the rotating frame). The angle  $\gamma$  between the effective electric field and the vector  $\boldsymbol{\omega}_1$  (or  $\boldsymbol{\omega}_2$ ) satisfies

$$\tan \gamma = \frac{3nZ}{2bv}. \quad (9)$$

Here  $v$  is the relative collision velocity and  $b$  is the impact parameter ( $\mathcal{L} = \mu bv$ ).

The second property is manifested in the fact that the precession is uniform in the effective time which coincides with the angle  $\Phi$ :

$$\Phi(t) = \int_{-\infty}^t \frac{\mathcal{L}}{\mu R^2(t')} dt'. \quad (10)$$

In quantum terms this means that the eigenstates for the projections  $\mathbf{I}_1 \boldsymbol{\omega}_1 / \omega_1$  and  $\mathbf{I}_2 \boldsymbol{\omega}_2 / \omega_2$  do not change in time. There are no transitions between these states during the collision,<sup>4)</sup> but in the course of the collision the eigenfunctions acquire the phase factors

$$\exp[i(n' + n'')\Omega], \quad (11)$$

where  $n'$  and  $n''$  are the eigenvalues for the projections of  $\mathbf{I}_1$  and  $\mathbf{I}_2$  on the axes  $\boldsymbol{\omega}_1$  and  $\boldsymbol{\omega}_2$  respectively, and

$$\Omega = \frac{\Delta\Phi}{\cos \gamma} = \Delta\Phi \sqrt{1 + \left(\frac{3nZ}{2bv}\right)^2}. \quad (12)$$

Here  $\Delta\Phi = \Phi(t \rightarrow \infty)$  is the angle of rotation of the internuclear axis in course of the collision; for rectilinear trajectories  $\Delta\Phi = \pi$ . It should be stressed that in general the present development does not require the assumption of the straight-line trajectories; conservation of the orbital momentum  $\mathcal{L}$  is sufficient. For example, replacing the Rydberg atom by a Rydberg ion (with some bare charge) one can incorporate in the theory the Coulomb trajectories of the colliding particles by simply substituting an appropriate angle  $\Delta\Phi(b)$ .

Now we discuss the physical assumptions used in the present scheme. The dipole approximation for the interaction is common to all theoretical papers on the subject.<sup>6-8</sup> The conditions of its applicability are discussed, for instance, in Ref. 6; see also Sec. 5 below. The scheme assumes exact degeneracy of the energy levels within the given  $n$ -manifold. In reality the degeneracy is somewhat lifted by various physical mechanisms; this effect can be taken into account in the quasihydrogenic approximation (see Ref. 8 and section 5).

The Stark levels belonging to adjacent  $n$ -manifolds (pseudo-)cross for  $R < \sqrt{3n^3Z}$ . However, the intershell ( $n$ -changing) transitions (neglected in the present scheme) generally become effective for substantial smaller internuclear separations. Indeed, the related Stark states correspond to an electron cloud shifted along the electric field and in opposite direction. Therefore the wavefunction overlap is small, which leads to small level splitting at the pseudocrossing. The pseudocrossings are passed diabatically unless the collision velocity is very small. We limit ourselves to these qualitative remarks, since the detailed estimates for intershell transitions could be the subject of a separate study.

### 3. QUANTUM TRANSITION AMPLITUDES

#### Parabolic basis

We start by considering the intrashell mixing in the simplest basis of states, namely, let the Rydberg atom initially be in the spherical  $(l_0, m_0)$  state. We are looking for the final state distributions over the quantum numbers  $i_1$  and  $i_2$  which are eigenvalues for the projections on the collision velocity axis of the vectors  $\mathbf{I}_1$  and  $\mathbf{I}_2$  respectively.

The propagation in time (up to the limit  $t \rightarrow \infty$  which gives the result of the collision) is reduced to purely geo-

metrical operations which are completely analogous to the precession picture in classical mechanics. The succession of operations is as follows:

(i) choose a standard parabolic (i.e.,  $i_1, i_2$ ) basis with some arbitrary axis and expand the initial electron wave function in this basis;

(ii) apply the operations of finite rotations in order to switch to the  $(n', n'')$  basis;

(iii) propagate in time by multiplying the  $(n', n'')$ -basis state vectors by the phase factors (11) (which corresponds to rotations around the  $\omega_1$  and  $\omega_2$  precession axes);

(iv) return to the original basis using the same (but inverted) finite rotations applied in reverse order.

The matrices of finite rotations are given by the well known Wigner functions.<sup>15</sup> The implementation of the scheme given above allowed Demkov *et al.*<sup>6</sup> to express the transition amplitudes in the  $(i_1, i_2)$ -basis as the product of four Wigner functions (two for each vector  $\mathbf{I}_1$  and  $\mathbf{I}_2$ ) and the phase factors, summed over two indices.<sup>5)</sup> Transformation to the spherical  $(l, m)$  basis requires additional coupling of the "angular momenta"  $\mathbf{I}_1$  and  $\mathbf{I}_2$  using the standard Clebsch–Gordan coefficients.

Thus, one has to perform three rotations for each vector  $\mathbf{I}_1$  and  $\mathbf{I}_2$ , which results in a formula containing at least four summation indices. The first simplification (used also by Abramov *et al.*<sup>18</sup>) stems from the fact that the product of several rotations can be represented as a single rotation. The rules to calculate the parameters of the latter rotation are known. For example, they are cited in the reference book by Varshalovich *et al.*;<sup>15</sup> we follow notations and conventions employed therein.

The resulting rotations are distinct for the vectors  $\mathbf{I}_1$  and  $\mathbf{I}_2$ . Namely, in the first case the rotation is characterized by the set of Euler angles  $\Omega_1 = \{\alpha_1, \beta_1, \gamma_{1E}\}$  defined by the relations

$$\begin{aligned} \cos \beta_1 &= \cos^2 \gamma \cos \Omega + \sin^2 \gamma, \quad \tan \alpha_1 = \tan \gamma_{1E} \\ &= \frac{1}{\sin \gamma} \cot \frac{\Omega}{2}, \end{aligned} \quad (13)$$

where  $\gamma$  and  $\Omega$  are the collision parameters introduced by Eqs. (9) and (12). Note the very simple and helpful expression

$$\sin \frac{\beta_1}{2} = \cos \gamma \sin \frac{\Omega}{2}. \quad (14)$$

For the vector  $\mathbf{I}_2$  the set of Euler angles  $\Omega_2 = \{\alpha_2, \beta_2, \gamma_{2E}\}$  is

$$\beta_2 = \beta_1, \quad \alpha_2 = \pi - \alpha_1, \quad \gamma_{2E} = \pi - \gamma_{1E}. \quad (15)$$

It is worth stressing that the effective electric field axis (i.e., essentially the collision velocity vector) is chosen as the Z-axis in the definition of the Euler angles adopted here. Of course, these rotations appear in both classical and quantum versions of the theory.

The quantum amplitude for the transition from the initial spherical  $(l_0, m_0)$  state into the final parabolic  $(i_1, i_2)$  state is represented as

$$f_{i_1 i_2} = \sum_{i'_1 i'_2} D_{i_1 i'_1}^j(\alpha_1, \beta_1, \gamma_{1E}) D_{i_2 i'_2}^j(\alpha_2, \beta_2, \gamma_{2E}) C_{j i'_1 i'_2}^{l_0 m_0}, \quad (16)$$

where we employ conventional notations for the Wigner functions  $D_{i_1 i'_1}^j(\alpha, \beta, \gamma)$  and Clebsch–Gordan coefficients  $C_{i_1 m_1 i_2 m_2}^{LM}$ , and  $j = (n-1)/2$ .

The subsequent development holds only if the Rydberg atom is initially in the  $s$ -state ( $l_0 = m_0 = 0$ ), whereupon the nonzero Clebsch–Gordan coefficients are exceedingly simple:

$$C_{j i j -i'}^{00} = (-1)^{j+i} \frac{1}{\sqrt{2j+1}} \delta_{ii'}. \quad (17)$$

Summation over one index is removed in the expression (16), with the result

$$\begin{aligned} f_{i_1 i_2} &= \frac{1}{\sqrt{2j+1}} \sum_{i'} (-1)^{j+i'} D_{i_1 i'}^j(\alpha_1, \beta_1, \gamma_{1E}) \\ &\quad \times D_{i_2 -i'}^j(\alpha_2, \beta_2, \gamma_{2E}) \\ &= \frac{1}{\sqrt{2j+1}} \exp(i\alpha_1 i_1 + i\alpha_2 i_2) \\ &\quad \times \sum_{i'} (-1)^{j+i} \exp(i\gamma_{1E} i' \\ &\quad - i\gamma_{2E} i') d_{i_1 i'}^j(\beta_1) d_{i_2 -i_2}^j(\beta_2). \end{aligned} \quad (18)$$

The latter transitions is carried out using the well-known relations

$$\begin{aligned} D_{i' i''}^j(\alpha, \beta, \gamma) &= \exp(i\alpha i') d_{i' i''}^j(\beta) \exp(i\gamma i''), \\ d_{i' i''}^j(\beta) &= d_{-i'' -i'}^j(\beta). \end{aligned} \quad (19)$$

The sum in the formula (18) corresponds to the product of two successive rotations which can be combined into a single rotation with new Euler angles. We employ the addition theorem for the Wigner functions which can be written as<sup>15</sup>

$$\begin{aligned} \sum_{i'} d_{i_1 i'}^j(\beta_1) d_{i_2 i'}^j(\beta_2) \exp(i\phi) \\ = \exp(i\alpha_0 i_1) d_{i_1 i_2}^j(\beta_0) \exp(i\gamma_0 i_2) \end{aligned} \quad (20)$$

with

$$\cot \alpha_0 = \cos \beta_1 \cot \phi + \cot \beta_2 \frac{\sin \beta_1}{\sin \phi}, \quad (21)$$

$$\cos \beta_0 = \cos \beta_1 \cos \beta_2 - \sin \beta_1 \sin \beta_2 \cos \phi, \quad (22)$$

$$\cot \gamma_0 = \cos \beta_2 \cot \phi + \cot \beta_1 \frac{\sin \beta_2}{\sin \phi}. \quad (23)$$

After some algebra a remarkably simple expression is obtained for the parameter  $\beta_0$  in terms of the dynamic angles  $\gamma, \Omega$ :

$$\sin \frac{\beta_0}{2} = \sin 2\gamma \sin^2 \frac{\Omega}{2}. \quad (24)$$

Thus we have obtained a final expression for the transition amplitude with a single Wigner function and without any summation:

$$F_{i_1 i_2} = \frac{(-1)^j}{\sqrt{2j+1}} \exp(i\alpha_1 i_1 + i\alpha_2 i_2 + i\alpha_0 i_1 - i\gamma_0 i_2) d_{i_1 - i_2}^j(\beta_0) = \frac{(-1)^j}{\sqrt{2j+1}} D_{i_1 - i_2}^j(\alpha_1 + \alpha_0, \beta_0, \gamma_0 - \alpha_2). \quad (25)$$

### Spherical basis

Generally the representation of the transition amplitude in terms of the final spherical  $l, m$  states is given by

$$F_{lm} = \sum_{i_1 i_2} C_{j i_1 j i_2}^{lm} F_{i_1 i_2}. \quad (26)$$

In order to carry out this summation we employ a rarely used representation for the Wigner function:<sup>19</sup>

$$D_{i_1 - i_2}^j(\tilde{\alpha}, \tilde{\beta}, \tilde{\gamma}) = \sum_{\lambda=|\tilde{l}_1 + \tilde{l}_2|}^{\lambda \leq 2j} (-1)^{\lambda + j - i_1} \times \sqrt{\frac{4\pi}{2j+1}} Y_{\lambda i_1 + i_2}(\Theta, \tilde{\Phi}) \chi_{\lambda}^j(\omega) C_{j i_1 j i_2}^{\lambda i_1 + i_2}. \quad (27)$$

Here the Euler angles  $\{\tilde{\alpha}, \tilde{\beta}, \tilde{\gamma}\}$  describe an arbitrary rotation of the three-dimensional frame; alternatively, the same transformation can be described<sup>15</sup> as a rotation through angle  $\omega$  around the axis characterized by the spherical angles  $\Theta, \tilde{\Phi}$ . The representations for the rotation are interrelated:<sup>15</sup>

$$\cos \frac{\omega}{2} = \cos \frac{\tilde{\beta}}{2} \cos \frac{\tilde{\alpha} + \tilde{\gamma}}{2}, \quad (28)$$

$$\tan \Theta = \tan \frac{\tilde{\beta}}{2} \left( \sin \frac{\tilde{\alpha} + \tilde{\gamma}}{2} \right)^{-1}, \quad (29)$$

$$\Phi = \frac{\pi}{2} + \frac{\tilde{\alpha} - \tilde{\gamma}}{2}. \quad (30)$$

In our problem the set of angles  $\{\omega, \Theta, \Phi\}$  is expressed in terms of important parameters (with the physical meaning discussed in the next section). Namely, after some cumbersome algebra we obtain quite simple expressions

$$\sin \frac{\omega}{2} = \epsilon_m, \quad \Theta = \frac{\pi}{2} - \zeta, \quad \tilde{\Phi} = 0, \quad (31)$$

$$\epsilon_m = 2 \sin \gamma \left| \sin \frac{\Omega}{2} \right| \sqrt{\cos^2 \gamma \sin^2 \frac{\Omega}{2} + \cos^2 \frac{\Omega}{2}},$$

$$\tan \zeta = \frac{1}{\cos \gamma} \cot \frac{\Omega}{2}. \quad (32)$$

The function  $\chi_{\lambda}^j(\omega)$  is the generalized character<sup>15</sup> for the irreducible representations of the rotation group expressed in Gegenbauer polynomials

$$\chi_{\lambda}^j(\omega) = (2\lambda)!! \sqrt{2j+1} \sqrt{\frac{(2j-\lambda)!}{(2j+\lambda+1)!}} \times \left( \sin \frac{\omega}{2} \right)^{\lambda} C_{2j-\lambda}^{\lambda+1} \left( \cos \frac{\omega}{2} \right). \quad (33)$$

Using the representation (27) we carry out summation over the indexes  $i_1$  and  $i_2$  with the final remarkably compact analytical expression for the transition amplitude

$$f_{(0,0) \rightarrow (l,m)}(b) = \frac{\sqrt{4\pi}}{2j+1} Y_{lm} \left( \frac{\pi}{2} - \zeta, 0 \right) \chi_l^j(\omega). \quad (34)$$

This is very useful even from the purely practical point of view, since the number of terms in the four-fold summation implied by formulae (16), (26) increases with  $n$  as  $n^4$ .

The total probability summed over the final state azimuthal quantum number  $m$  is

$$\sum_{m=-l}^l |f_{(0,0) \rightarrow (l,m)}(b)|^2 = \frac{2l+1}{(2j+1)^2} \chi_l^j(\omega). \quad (35)$$

### 4. CLASSICAL LIMIT

Since the special functions entering formulae (25), (34) and (35) obey well known differential equations, it is easy to obtain semiclassical approximations for the transition amplitudes of various levels of sophistication. Below we are interested in the crudest version of this approximation. This allows us to trace the transition from the exact quantum solution to the classical approximation introduced by Kazansky and Ostrovsky<sup>8</sup> within a quite different formalism. The related formulae for the special functions are not cited in the mathematical literature, being probably regarded as too crude. We can easily derive them by invoking the well-known differential equations which can be conveniently presented in the form

$$\left[ -\frac{d^2}{d\beta_0^2} + \frac{i_1^2 - 2i_1 i_2 \cos \beta_0 + i_2^2 + 1/4}{\sin^2 \beta_0} - \left( j + \frac{1}{2} \right)^2 \right] \times (\sqrt{\sin \beta_0} d_{i_1 i_2}^j(\beta_0)) = 0, \quad (36)$$

$$\left[ -\frac{d^2}{d\omega^2} + \frac{l(l+1)}{4 \sin^2(\omega/2)} - \left( j + \frac{1}{2} \right)^2 \right] \left( \sin \frac{1}{2} \omega \chi_{\lambda}^j(\omega) \right) = 0, \quad (37)$$

$$\left[ -\frac{d^2}{d\theta} + \frac{m^2}{\sin^2 \theta} + \left( l + \frac{1}{2} \right)^2 \right] (\sqrt{\sin \theta} Y_{lm}(\theta, \varphi)) = 0. \quad (38)$$

All these equations have the form of the conventional one-dimensional Schrödinger equation. For the latter the crudest (semi) classical approximation for the probability density reads:

$$|\psi(x)|^2 \sim \frac{1}{v(x)}, \quad v(x) = \sqrt{2[E - V(x)]}, \quad (39)$$

where  $v(x)$  is the classical velocity at the point  $x$  for the electron moving in the potential  $V(x)$ . It corresponds to averaging over all quantum oscillations and neglecting tunneling. Applying this approach we obtain after some simple transformations, normalization and reparametrization<sup>6)</sup>

$$|d_{i_1-i_2}^j(\beta_0)|^2 \approx \frac{1}{\pi(2j+1)\sin\beta_0} \times \frac{1}{\sqrt{1-\mu^2/\sin^2(\beta_0/2)-\alpha^2/\cos^2(\beta_0/2)}}, \quad (40)$$

$$|\chi_\lambda^j(\omega)|^2 \approx \frac{2j+1}{2\sin(\omega/2)\sqrt{(2j+1)^2\sin^2(\omega/2)-l(l+1)}}, \quad (41)$$

$$|Y_{lm}(\theta, \varphi)|^2 \approx \frac{(l+1/2)\sin\theta}{2\pi^2\sqrt{(l+1/2)^2\sin^2\theta-m^2}}, \quad (42)$$

where

$$\mu = \frac{i_1+i_2}{n} = \frac{m}{n}, \quad \alpha = \frac{i_1-i_2}{n} = \frac{n_1-n_2}{n}. \quad (43)$$

The quantum transition probabilities are defined as

$$P_{mn_1-n_2}^q(b) \equiv |F_{i_1 i_2}|^2 = \frac{1}{2j+1} d_{i_1-i_2}^j(\beta_0)^2, \quad (44)$$

$$P_{0 \rightarrow l}^q(b) \equiv \sum_{m=-l}^l |f_{(0,0) \rightarrow (l,m)}(b)|^2 = \frac{2l+1}{(2j+1)^2} \chi_l^j(\omega), \quad (45)$$

$$P_{(0,0) \rightarrow (l,m)}^q(b) \equiv |f_{(0,0) \rightarrow (l,m)}(b)|^2 = \frac{4\pi}{(2j+1)^2} Y_{lm}\left(\frac{\pi}{2}, 0\right)^2 \chi_l^j(\omega). \quad (46)$$

Their crude (semi-) classical counterparts are

$$P^{sc}(m, n_1-n_2; b) = \frac{1}{\pi n^2 \mu_m \alpha_m} \frac{1}{\sqrt{1-\mu^2/\mu_m^2-\alpha^2/\alpha_m^2}}, \quad (47)$$

$$P^{sc}(l; b) = \frac{\epsilon}{n \epsilon_m \sqrt{\epsilon_m^2 - \epsilon^2}}, \quad (48)$$

$$P^{sc}(l, m; b) = \frac{1}{\pi n^2} \frac{\epsilon}{\sqrt{\epsilon_m^2 - \epsilon^2} \sqrt{\mu_m^2 \epsilon^2 - \epsilon_m^2 \mu^2}}, \quad (49)$$

where

$$\mu_m = \sin \frac{1}{2} \beta_0, \quad \alpha_m = \cos \frac{1}{2} \beta_0, \quad (50)$$

the classical orbital angular momentum is  $L=l+1/2$ , and  $\epsilon=L/n$ . The formulae (40)–(42) and (47)–(49) are valid provided the expressions under square roots are positive; otherwise the right hand sides have to be put equal to zero. Because of this property the parameters  $\epsilon_m$ ,  $\mu_m$  and  $\alpha_m$  have

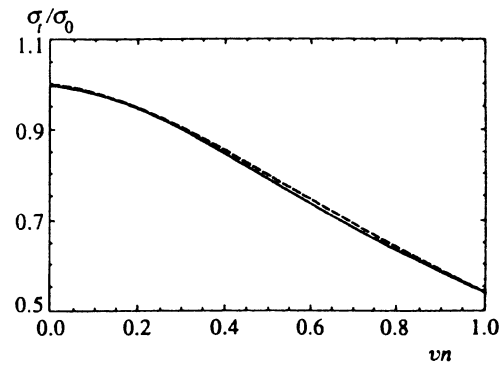


FIG. 1. Total cross section of intrashell transitions  $\sigma$ , related to its low-velocity limit  $\sigma_0$ . Collision of Na(26d) atom with an ion is considered in the quasihydrogenic approximations (see text). The reduced velocity  $vn$  is the ratio between the collision velocity  $v$  and the typical Rydberg electron velocity  $1/n$ .

clear physical meaning, being related to the largest values of the variables  $\epsilon$ ,  $\mu$  and  $\alpha$  attained within the classical approximation.

Consider now formula (45) and its approximation (48) as an example. These expressions give the impact-parameter-dependent transition probability for the integer quantum number  $l$ . In slightly different terms it can be understood as the final state distribution over the (integer)  $l$ . The latter interpretation can be extended to a purely classical description where the variables  $l$  and  $m$  vary continuously. Comparison shows that the right hand sides of the formulae (47)–(49) coincide with the distribution obtained within our previous classical analysis.<sup>8</sup>

Although some direct connection between the classical and quantum distribution functions is established in this way, it is inappropriate for realistic quantitative applications. This is seen already from the fact that the approximations (47)–(49) can exceed unity, thus violating the unitarity constraint. The appropriate relation between the classical and quantum results is given by the binning procedure<sup>5</sup> used in the standard CTMC and in Ref. 8. According to it one has to identify, for instance,

$$P_{0 \rightarrow l}^{cl}(b) = \int_l^{l+1} P^{sc}(L; b) dL, \quad (51)$$

which certainly restores unitarity. The plain prescription  $L=l+1/2$  can be understood as a result of the simplest estimate for this integral. Similar binning formulae could be written down for quantum numbers other than  $l$ .

## 5. TRANSITION CROSS SECTIONS

Integration over impact parameters gives divergent cross sections for the dipole-allowed transitions ( $|\Delta l|=1$ ). However this is true only in the case of exact degeneracy of levels within the given  $n$  manifold. In fact, this degeneracy is broken for realistic Rydberg atoms. For the hydrogen atom (or one-electron hydrogenlike ions) the degeneracy is lifted by the fine structure level splitting and Lamb shift (see the paper by Chibisov<sup>20</sup> who considered the case  $n=2$ ). In the multi-electron atoms the effective potential seen by the excited

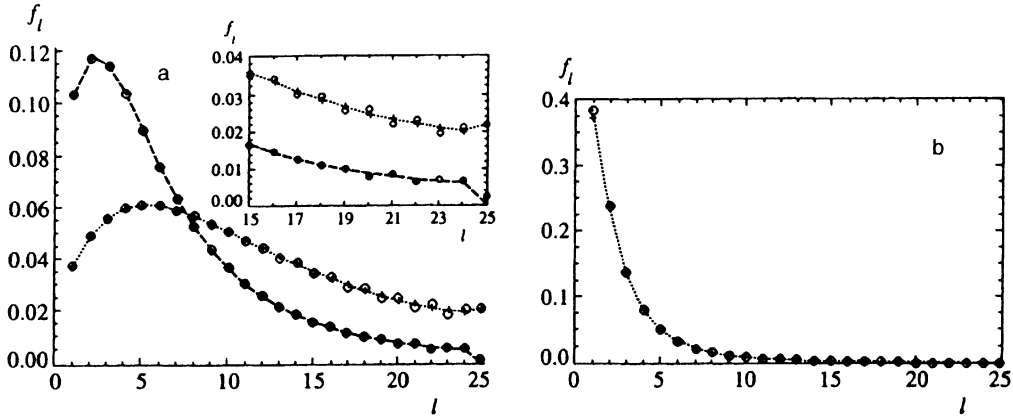


FIG. 2. Reduced cross sections (or fractional populations)  $f_l$  for the final states of Na(26*l*) atom in the quasihydrogenic approximation for various reduced collision velocities  $\nu n$ . The quantum results are shown by open circles, the classical (pseudo-) CTMC results are presented by crosses (for  $\nu n=0.1$  (a) and  $\nu n=0.6$  (b)) and small closed circles ( $\nu n=0.2$  (a)). The symbols are joined by smooth lines for convenience. The inset shows details of the relation between quantum and classical results for large  $l$ .

electron differs from the Coulomb potential. Typically the non-Coulomb core produces energy level splittings which are much larger than those due to the relativistic effects.

Bearing in mind application to the intrashell transitions in Na(*nd*) explored in the experiment<sup>2</sup> ( $n=26$  and  $28$ ), we use the quasihydrogenic approximation to mimic the effect of the non-Coulomb core in the Rydberg atom as described in Ref. 8. Briefly, the strong intrashell level mixing is operative when the linear Stark shift of the outermost levels in the manifold ( $\sim 3n^2Z/(2R^2)$ ) exceeds the level splitting produced by the core ( $\sim \delta n^3$ , where  $\delta$  is the quantum defect). From this we obtain the expression for the critical internuclear separation  $R_{\max} = \sqrt{3n^5Z/2\delta}$ . In the subsequent model calculation we take the value  $\delta_d=0.0135$  which is the quantum defect for Na(*nd*) states. It is assumed that the intrashell mixing is operative only for the part of the nuclear trajectory lying inside the  $R_{\max}$ -sphere. This leads to the following expression for the effective rotation angle of the internuclear axis:

$$\Delta\Phi = 2 \arcsin(b/R_{\max})(b < R_{\max}), \quad \Delta\Phi = 0(b > R_{\max}). \quad (52)$$

For low  $b$  the dipole approximation for the interaction becomes invalid. We define this boundary roughly as  $b_{\min}=4n^2$ ; the cross sections are fairly insensitive to it.<sup>8</sup>

The cross section calculation requires a single numerical integration over the impact parameter  $b$ . The results are presented below with the parameters chosen as described. Figure 1 shows the total cross section  $\sigma_t$  for the intrashell transitions. For low  $\nu n$  this cross section approaches the limiting value  $\sigma_0=\pi(R_{\max}^2-b_{\min}^2)/2$ . This implies that almost all trajectories penetrating the  $R_{\max}$ -sphere lead to  $l$ -mixing. For our particular choice of the quantum defect  $\delta$  we obtain  $\sigma_0=2872\pi n^4$ , which takes the huge value  $\sigma_0=11.55 \times 10^{-8}$  cm<sup>2</sup> for  $n=26$  employed in experiment.<sup>2</sup> For higher  $\nu n$  the ratio  $\sigma_t/\sigma_0$  decreases.

Although the formulae (47)–(49) give a crude approximation for the dependence of the transition probabilities on the impact parameter, the difference between the quantum

and classical results for the quantities integrated over  $b$  proves to be very small. For  $\sigma_t$  this is seen from Fig. 1. This is also the case for the cross sections  $\sigma_{(0,0) \rightarrow (\nu\nu')}$  describing transitions into individual quantum states  $(\nu, \nu')$ . It is convenient to use the reduced cross sections defined as

TABLE I. Reduced cross sections  $f_{\Delta l}$  for the process Na(26*d*) + Na<sup>+</sup> → Na(26*l* + 2Δ*l*) + Na<sup>+</sup> at various values of the relative collision velocity  $\nu n$ . In each block the upper figure is the present quantum theory within the quasihydrogenic approximation for Na; the next figure is the same but in our (pseudo-) CTMC scheme;<sup>8</sup> the lowest figure is the experimental data by Sun and MacAdam.<sup>2</sup>

$\nu n$	$\Delta l = 1$	$\Delta l = 2$	$\Delta l = 3$
0.1	0.0373	0.0489	0.0556
	0.0373	0.0489	0.0558
	0.111(15)	0.102(19)	
0.2	0.103	0.117	0.114
	0.103	0.118	0.115
	0.155(20)	0.142(17)	
0.3	0.179	0.173	0.143
	0.179	0.174	0.144
	0.205(28)	0.135(28)	0.078(23)
0.4	0.252	0.208	0.150
	0.254	0.211	0.150
	0.233(23)	0.193(27)	0.090(30)
0.5	0.317	0.227	0.146
	0.324	0.229	0.144
	0.322(27)	0.183(57)	0.119(40)
0.6	0.373	0.236	0.137
	0.384	0.236	0.134
	0.384(22)	0.226(25)	0.104(25)
0.7	0.421	0.238	0.128
	0.436	0.236	0.123
	0.466(28)	0.205(45)	0.096(28)
0.9	0.497	0.233	0.111
	0.518	0.225	0.105
	0.566(36)	0.172(33)	0.081(20)

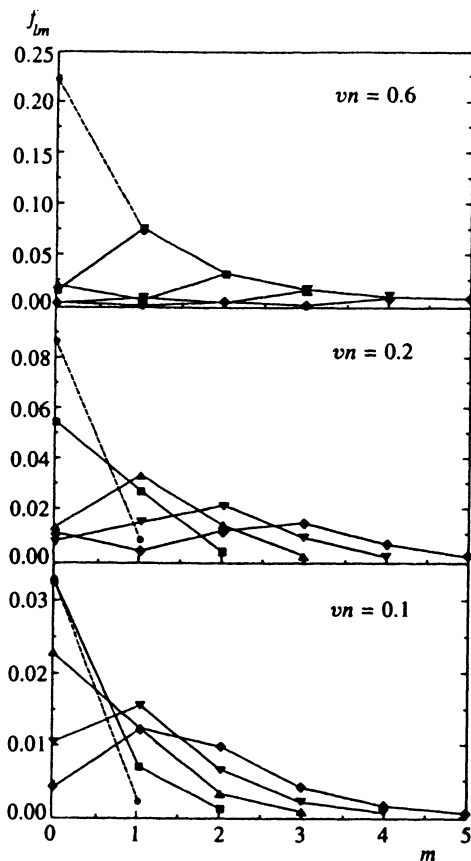


FIG. 3. Reduced cross sections  $f_{lm}$  for the same process as in Fig. 2 in the low- $l$  domain for different reduced collision velocities  $vn$ . The symbols correspond to various values of the final orbital momentum  $l$ : crosses— $l=1$ ; boxes— $l=2$ ; triangles up— $l=3$ ; triangles down— $l=4$ ; diamonds— $l=5$ .

$$f_{\nu\nu'} = \sigma_{(0,0) \rightarrow (\nu\nu')} / \sigma_l. \quad (53)$$

For the final  $l$ -states these quantities coincide with the fractional populations introduced by Sun and MacAdam.<sup>2</sup>

The reduced cross sections  $f_l$  are shown in Fig. 2 for some values of the reduced velocity  $vn$ . For low  $vn$  the final state distributions form a very broad pattern. Very roughly it can be described as a uniform (in terms of  $l$ ) population of all available quantum states ( $l \leq n-1$ ). Note that this distribution is far from the statistical one (the latter presupposes linear growth of  $f_l$  with  $l$ ). For large  $vn$  the dipole-allowed transitions ( $|\Delta l|=1$ ) dominate. Nevertheless, even for  $vn$  close to 1 the transitions with larger  $|\Delta l|$  remain appreciable. The quantum and classical results almost coincide on the scale of Fig. 2. The small differences are more noticeable for large  $l$ . Interestingly, the quantum results show shallow oscillations relative to the smoother classical curve (Fig. 2, inset).

Table I shows comparison of the present results with the experimental data for  $n=26$  by Sun and MacAdam.<sup>2</sup> The agreement is quite good. The very small difference between quantum and classical results has to be stressed again. This allows us to omit here comparison with the experimental

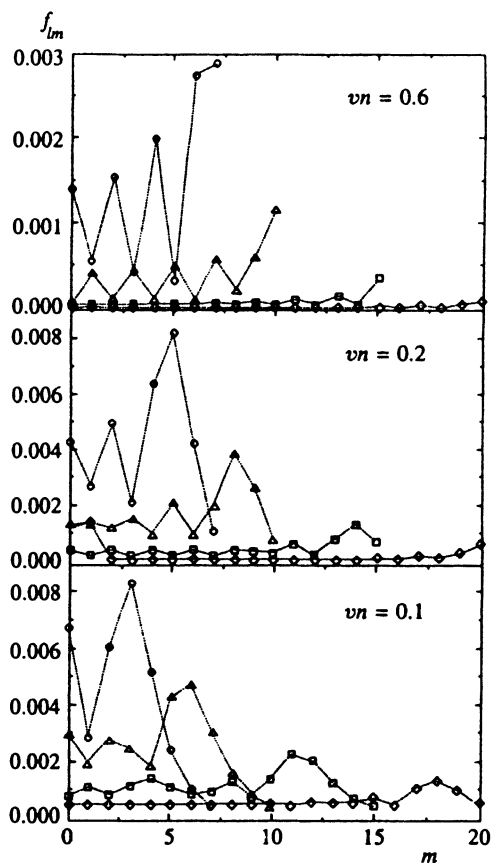


FIG. 4. Same as in the Fig. 3, but for some representative large- $l$  states: circles— $l=7$ ; triangles— $l=10$ ; boxes— $l=15$ ; diamonds— $l=20$ .

data for  $n=28$  since for the classical theory the discussion was already presented elsewhere.<sup>8</sup>

Typical distributions over the azimuthal quantum numbers are shown in Figs. 3 and 4. For small  $l$  the distributions are strongly peaked at  $m=0$ . As  $l$  increases, the  $m$ -distributions become more broad; oscillatory patterns can be noticed. For large  $l$  the  $m$ -distributions are close to uniform with a small maximum at the higher  $m$  side.

To summarize, in the present paper we have found a compact expression for the quantum transition amplitude and studied its semiclassical limit. This is equivalent to the explicit solution of the close-coupling problem for  $n^2$  states in the fixed- $n$  manifold. The underlying reason for this result lies in efficient use of the Fock  $O(4)$  symmetry group for the hydrogen atom. The classical limit of the quantum solution is studied in detail. Very good agreement is found between the quantum and classical results for the transition cross sections which justifies the binning procedure used in CTMC calculations. Good agreement with the recent experimental data is achieved.

Part of this work was carried out during the visit of one of the authors (V.N.O.) to the University of Aarhus, Denmark. The hospitality of this institution and useful discussions with K. Taulbjerg are gratefully acknowledged.

- <sup>1</sup>Note however that the formulae (13)–(18) below are valid for the general case.
- <sup>2</sup>Atomic units are used throughout.
- <sup>3</sup>For an interesting extension of this approach see the recent paper by Cavagnero.<sup>10</sup>
- <sup>4</sup>Because of this property these states were termed dynamic states by Demkov *et al.*<sup>6</sup>
- <sup>5</sup>This approach was applied to the line broadening problem (see Ref. 16) and collisions in an external magnetic field,<sup>17</sup> additional references can be found in Refs. 3, 8.
- <sup>6</sup>The additional term  $1/4$  in Eq. (36) has to be omitted in the semiclassical limit.
- 
- <sup>1</sup>I. L. Beigman and V. S. Lebedev, Phys. Rep. **250**, 95 (1995).
- <sup>2</sup>X. Sun and K. B. MacAdam, Phys. Rev. A **47**, 3913 (1993).
- <sup>3</sup>A. K. Kazansky, J. Phys. B **25**, L381 (1992); A. K. Kazansky and P. Roncin, J. Phys. B **27**, 5537 (1994).
- <sup>4</sup>W. G. Scherzer, H. L. Selzle, E. W. Schlag, and R. D. Levine, Phys. Rev. Lett. **72**, 1435 (1994); A. Mühlpfordt, U. Even, E. Rabani, and R. D. Levine, Phys. Rev. A **51**, 3922 (1995).
- <sup>5</sup>R. L. Becker and A. D. MacKellar, J. Phys. B **17**, 3923 (1984).
- <sup>6</sup>Yu. N. Demkov, V. N. Ostrovsky, and E. A. Solov'ev, Zh. Eksp. Teor. Fiz. **66**, 125 (1974) [Sov. Phys. JETP **39**, 57 (1974)].
- <sup>7</sup>I. L. Beigman and M. I. Syrkin, Zh. Eksp. Teor. Fiz. **89**, 400 (1985) [Sov. Phys. JETP **62**, 226 (1985)].
- <sup>8</sup>A. K. Kazansky and V. N. Ostrovsky, Phys. Rev. A **52**, R1811 (1995); J. Phys. B **29**, 3651 (1996).
- <sup>9</sup>V. Fock, Z. Phys. **98**, 145 (1935).
- <sup>10</sup>M. J. Cavagnero, Phys. Rev. A **52**, 2865 (1995).
- <sup>11</sup>P. S. Epstein, Phys. Rev. A **22**, 202 (1923).
- <sup>12</sup>W. Pauli, Z. Phys. **36**, 336 (1926).
- <sup>13</sup>M. Born, *Mechanics of the Atom*, New York, Ungar (1960).
- <sup>14</sup>Yu. N. Demkov, B. S. Monoszon, and V. N. Ostrovsky, Zh. Eksp. Teor. Fiz. **57**, 1431 (1969) [Sov. Phys. JETP **30**, 775 (1970)].
- <sup>15</sup>D. A. Varshalovich, A. N. Moskalev, and V. K. Khersonskii, *Kvantovaya Teoriya Uglovogo Momenta*, Leningrad, Nauka (1975). (English Translation: *Quantum Theory of Angular Momentum*, Singapore, World Scientific (1988)).
- <sup>16</sup>V. S. Lisitza and G. V. Sholin, Zh. Eksp. Teor. Fiz. **61**, 912 (1971) [Sov. Phys. JETP **34**, 484 (1972)].
- <sup>17</sup>K. Sakimoto, J. Phys. B **25**, 3641 (1992).
- <sup>18</sup>V. A. Abramov, F. F. Baryshnikov, and V. S. Lisitsa, Zh. Eksp. Teor. Fiz. **74**, 897 (1978) [Sov. Phys. JETP **47**, 469 (1978)].
- <sup>19</sup>M. S. Marinov, Yadernaya Fizika **5**, 1321 (1967) [Sov. J. Nucl. Phys. **5**, 943 (1967)].
- <sup>20</sup>M. I. Chibisov, Optika i Spektrosk. **27**, 9 (1969) [Opt. Spectrosc. (USSR) **27**, 4 (1969)].

Published in English in the original Russian journal. Reproduced here with stylistic changes by the Translation Editor.